



# Free Vibration Analysis of Waves in a Microstretch Viscoelastic Layer

R. Kumar and G. Partap

**Abstract :** The free vibration analysis of waves in a homogeneous isotropic microstretch viscoelastic layer subjected to stress-free conditions is investigated. Mathematical modeling of the problem of obtaining dispersion curves for microstretch viscoelastic layer leads to coupled differential equations. The mathematical model has been simplified by using the Helmholtz decomposition technique and the resulting equations have been solved by using variable separable method to obtain the secular equations for both symmetric and skew-symmetric wave mode propagation. The special cases such as short wavelength and regions of secular equations are deduced and discussed. The dispersion curves, amplitudes of displacement components, microrotation and microstretch for symmetric and skew-symmetric modes are computed numerically and presented graphically. Results of some earlier workers have been deduced as particular cases.

**Keywords :** Microstretch viscoelastic layer; Secular equations; Phase velocity; Attenuation coefficients

**2000 Mathematics Subject Classification :** 74A; 74B; 74F; 74J; 74K (2000 MSC)

## 1 Introduction

The concept of microcontinuum proposed by Eringen [4] can take into account the microstructure effects while the theory itself is still a continuum formulation. The first grade micro-continuum consists a hierarchy of

theories, namely, micropolar, microstretch and micromorphic depending on how much microdegrees of freedom are incorporated. These high order continuum theories are considered to be potential tools to model the behavior of the material with a complicated microstructure. For example, in the case of foam composite, when the size of the reinforced phase is comparable to the intrinsic length scale of the foam, in this situation, the microstructure of the foam must be taken into account to some degree, so a high order continuum model must be assigned for the foam matrix. The same remains true for nanocomposites, since the scale of the reinforced phase is so small, the surrounding matrix can not be homogenized as a simple material (Cauchy medium), some intrinsic microstructures of the matrix must be considered in a proper continuum model.

Microstretch [2, 3] theory is a generalization of the micropolar theory, for such a material, a homogeneous stretch microdeformation is added to every particle i.e. besides the translation and rigid rotation, each particle can have an independently breathe - like degree of freedom. Such a generalized media can catch more detailed information about the microdeformation inside a material point. The material points of microstretch solids can stretch and contract independently of their translations and rotations. The microstretch continua are used to characterize composite materials and various porous media.

Liu and Hu [24] investigated the inclusion problem of microstretch. Svanadze [8] constructed fundamental solution of the system of equations of steady oscillations in the theory of microstretch elastic solids. De Cicco [22] investigated the stress concentration effects in microstretch elastic bodies. Kumar, Singh and Chadha [14] discussed the axisymmetric problem in microstretch. Kumar, Singh and Chadha [15] investigated plane strain problem in microstretch elastic solid. Kumar and Partap [17] investigated reflection of plane waves in a heat flux dependent microstretch thermoelastic solid half spaces.

Eringen [1] extended the theory of micropolar elasticity to obtain linear constitutive theory for micropolar material possessing internal friction. A problem on micropolar viscoelastic waves has been discussed by McCarthy and Eringen [7]. Biswas et al. [9] studied the axisymmetric problems of wave propagation under the influence of gravity in a micropolar viscoelastic semi-infinite medium when a time varying axisymmetric loading has been applied on the surface of the medium. De Cicco and Nappa [21] discussed the problem of Saint Venant's principle for micropolar viscoelastic bodies. Kumar and Singh [12] studied reflection of plane waves at a planar vis-

coelastic micropolar interface.

EI - Karamany [23] studied uniqueness and reciprocity theorems in a generalized linear micropolar thermoviscoelasticity. Kumar et al. [11] studied Lamb's plane problem in a micropolar viscoelastic half-space with stretch. Kumar [13] discussed wave propagation in micropolar viscoelastic generalized thermoelastic solid. Kumar and Singh [16] studied elastodynamics of an axisymmetric problem in microstretch viscoelastic solid. Kumar and Partap [19] discussed analysis of free vibrations for Rayleigh Lamb waves in a micropolar viscoelastic plate. Kumar and Sharma [20] investigated propagation of waves in micropolar viscoelastic generalized thermoelastic solids having interfacial imperfections.

The present investigation is aimed to study the free vibration analysis of waves in an infinite homogeneous, isotropic microstretch viscoelastic layer of thickness  $2d$ .

## 2 Basic Equations

The equations of motion and the constitutive relations in a microstretch elastic solid without body forces, body couples and stretch force given by Eringen [4] are

$$(\lambda + 2\mu + K)\nabla(\nabla \cdot \vec{u}) - (\mu + K)\nabla \times \nabla \times \vec{u} + K\nabla \times \vec{\phi} + \lambda_0 \nabla \phi^* = \rho \frac{\partial^2 \vec{u}}{\partial t^2}, \quad (2.1)$$

$$(\alpha + \beta + \gamma)\nabla(\nabla \cdot \vec{\phi}) - \gamma \nabla \times (\nabla \times \vec{\phi}) + K\nabla \times \vec{u} - 2K\vec{\phi} = \rho j \frac{\partial^2 \vec{\phi}}{\partial t^2}, \quad (2.2)$$

$$\alpha_0 \nabla^2 \phi^* - \lambda_1 \phi^* - \lambda_0 \nabla \cdot \vec{u} = \frac{1}{2} \rho j_0 \frac{\partial^2 \phi^*}{\partial t^2}, \quad (2.3)$$

$$t_{ij} = (\lambda_0 \phi^* + \lambda u_{r,r}) \delta_{ij} + \mu (u_{i,j} + u_{j,i}) + K (u_{j,i} - \epsilon_{ijr} \phi_r), \quad (2.4)$$

$$m_{ij} = \alpha \phi_{r,r} \delta_{ij} + \beta \phi_{i,j} + \gamma \phi_{j,i} + b_0 \epsilon_{mji} \phi_{,m}^*, \quad (2.5)$$

$$\lambda_i^* = \alpha_0 \phi_{,i}^* + b_0 \epsilon_{ijm} \phi_{j,m} \quad (2.6)$$

Assuming the viscoelastic nature of the material described by Kumar and Singh [16] model of linear viscoelasticity, we replace the microstretch elastic constants  $\lambda, \mu, K, \alpha, \beta, \gamma, \alpha_0, \lambda_0, \lambda_1, b_0$  by  $\lambda_I, \mu_I, K_I, \alpha_I, \beta_I, \gamma_I, \alpha_{0I}, \lambda_{0I}, \lambda_{1I}, b_{0I}$  where

$$\lambda_I = \lambda + \lambda_v \frac{\partial}{\partial t}, \mu_I = \mu + \mu_v \frac{\partial}{\partial t}, K_I = K + K_v \frac{\partial}{\partial t}, \alpha_I = \alpha + \alpha_v \frac{\partial}{\partial t}, \beta_I = \beta + \beta_v \frac{\partial}{\partial t},$$

$$\gamma_I = \gamma + \gamma_v \frac{\partial}{\partial t}, \alpha_{0I} = \alpha_0 + \alpha_{0v} \frac{\partial}{\partial t}, \lambda_{0I} = \lambda_0 + \lambda_{0v} \frac{\partial}{\partial t}, \lambda_{1I} = \lambda_1 + \lambda_{1v} \frac{\partial}{\partial t},$$

$$b_{0I} = b_0 + b_{0v} \frac{\partial}{\partial t}.$$

And  $\lambda_v, \mu_v, K_v, \alpha_v, \beta_v, \gamma_v, \alpha_{0v}, \lambda_{0v}, \lambda_{1v}, b_{0v}$  are viscosity coefficients in Eqs. (2.1) - (2.6), we obtain

$$(\lambda_I + 2\mu_I + K_I)\nabla(\nabla \cdot \vec{u}) - (\mu_I + K_I)\nabla \times \nabla \times \vec{u} + K_I\nabla \times \vec{\phi} + \lambda_{0I}\nabla\phi^* = \rho \frac{\partial^2 \vec{u}}{\partial t^2}, \quad (2.7)$$

$$(\alpha_I + \beta_I + \gamma_I)\nabla(\nabla \cdot \vec{\phi}) - \gamma_I\nabla \times (\nabla \times \vec{\phi}) + K_I\nabla \times \vec{u} - 2K_I\vec{\phi} = \rho j \frac{\partial^2 \vec{\phi}}{\partial t^2}, \quad (2.8)$$

$$\alpha_{0I}\nabla^2\phi^* - \lambda_{1I}\phi^* - \lambda_{0I}\nabla \cdot \vec{u} = \frac{1}{2}\rho j_0 \frac{\partial^2 \phi^*}{\partial t^2}, \quad (2.9)$$

$$t_{ij} = (\lambda_{0I}\phi^* + \lambda_I u_{r,r})\delta_{ij} + \mu_I(u_{i,j} + u_{j,i}) + K_I(u_{j,i} - \epsilon_{ijr}\phi_r), \quad (2.10)$$

$$m_{ij} = \alpha_I\phi_{r,r}\delta_{ij} + \beta_I\phi_{i,j} + \gamma_I\phi_{j,i} + b_{0I}\epsilon_{mji}\phi_{,m}^*, \quad (2.11)$$

$$\lambda_i^* = \alpha_{0I}\phi_{,i}^* + b_{0I}\epsilon_{ijm}\phi_{j,m} \quad (2.12)$$

where  $\lambda, \mu, \alpha, \beta, \gamma, K, \alpha_0, \lambda_0, \lambda_1, b_0$  are material constants,  $\rho$  is the density,  $j$  is the microinertia,  $j_0$  is the microinertia of microelement,  $t_{ij}$  components of stress tensor,  $m_{ij}$  components of couple stress tensor,  $\vec{u} = (u_1, u_2, u_3)$  is the displacement vector,  $\vec{\phi} = (\phi_1, \phi_2, \phi_3)$  is the microrotation vector,  $\lambda_i^*$  is the microstress tensor,  $\phi^*$  is the scalar point microstretch function, and  $\delta_{ij}$  is Kronecker delta,

The comma notation denotes spatial derivatives.

### 3 Formulation of the Problem

We consider a homogeneous isotropic microstretch viscoelastic layer of thickness  $2d$ . The origin of the coordinate system  $(x, y, z)$  is taken on the middle surface of the layer and  $z$  - axis normal to it along the thickness as illustrated in Fig. 1.

For two dimensional problem, we take

$$\vec{u} = (u_1, 0, u_3) \text{ and } \vec{\phi} = (0, \phi_2, 0)$$

We define the non-dimensional quantities

$$x' = \frac{\omega^* x}{c_1}, z' = \frac{\omega^* z}{c_1}, u'_1 = \frac{\omega^*}{c_1} u_1, u'_3 = \frac{\omega^*}{c_1} u_3, t' = \omega^* t, \phi'_2 = \frac{\omega^{*2} j}{c_1^2} \phi_2,$$

$$\begin{aligned}\phi^{*'} &= \frac{\omega^{*2}j}{c_1^2}\phi^*, \omega^{*2} = \frac{K_I}{\rho j}, t'_{ij} = \frac{1}{\lambda_I}t_{ij}, m'_{ij} = \frac{\omega^*m_{ij}}{\lambda_I c_1}, \lambda_i^{*'} = \frac{\omega^*\lambda_i^*}{c_1\lambda_I}, p = \frac{K_I}{\rho c_1^2}, \\ \delta^2 &= \frac{c_2^2}{c_1^2}, \delta_2^2 = \frac{c_1^2}{c_4^2}, \delta_3^2 = \frac{\lambda_{0I}}{K_I}, \delta^{*2} = \frac{K_I}{\rho c_4^2}, \delta_4^2 = \frac{\lambda_{1I}c_1^2}{\alpha_{0I}\omega^{*2}}, \delta_5^2 = \frac{\lambda_{0I}j}{\alpha_{0I}}, \delta_6^2 = \frac{\rho c_1^2 j_0}{2\alpha_{0I}}.\end{aligned}\quad (3.1)$$

where  $c_1^2 = \frac{\lambda_I + 2\mu_I + K_I}{\rho}$ ,  $c_2^2 = \frac{\mu_I + K_I}{\rho}$ ,  $c_4^2 = \frac{\gamma_I}{\rho j}$ ,  $\omega^*$  is the characteristic frequency of the medium,  $c_1$  and  $c_2$  are respectively longitudinal and shear wave velocity in the medium.

Introducing the velocity potential functions  $\phi$  and  $\psi$  through the relations

$$u_1 = \frac{\partial\phi}{\partial x} + \frac{\partial\psi}{\partial z}, u_3 = \frac{\partial\phi}{\partial z} - \frac{\partial\psi}{\partial x}, \quad (3.2)$$

and using Eqs. (3.1) - (3.2) in Eqs. (2.7) - (2.9) and after suppressing the primes for convenience, we obtain

$$\nabla^2\phi - \frac{\partial^2\phi}{\partial t^2} + \delta_3^2\phi^* = 0, \quad (3.3)$$

$$\nabla^2\psi - \frac{\phi_2}{\delta^2} - \frac{1}{\delta^2}\frac{\partial^2\psi}{\partial t^2} = 0, \quad (3.4)$$

$$\delta^{*2}\nabla^2\psi = \delta_2^2\frac{\partial^2\phi_2}{\partial t^2} + 2\delta_2^2\phi_2 - \nabla^2\phi_2, \quad (3.5)$$

$$\nabla^2\phi^* - \delta_4^2\phi^* - \delta_5^2\nabla^2\phi - \delta_6^2\frac{\partial^2\phi^*}{\partial t^2} = 0, \quad (3.6)$$

where

$$\nabla^2 = \frac{\partial^2}{\partial x^2} + \frac{\partial^2}{\partial z^2}$$

### 3.1 Boundary Conditions

The non-dimensional mechanical boundary conditions at  $z = \pm d$  are given by

$$t_{33} = 0, t_{31} = 0, m_{32} = 0, \lambda_3^* = 0, \quad (3.7)$$

where

$$t_{33} = \lambda_{0I}\phi^* + (\lambda_I + 2\mu_I + K_I)\frac{\partial u_3}{\partial z} + \lambda_I\frac{\partial u_1}{\partial x},$$

$$t_{31} = \mu_I\left(\frac{\partial u_1}{\partial z} + \frac{\partial u_3}{\partial x}\right) + K_I\left(\frac{\partial u_1}{\partial z} - \phi_2\right),$$

$$m_{32} = \gamma_I \frac{\partial \phi_2}{\partial z} + b_{0I} \frac{\partial \phi^*}{\partial x},$$

$$\lambda_3^* = \alpha_{0I} \frac{\partial \phi^*}{\partial z} - b_{0I} \frac{\partial \phi_2}{\partial x}.$$

## 4 Formal solution of the problem

We assume the solutions of Eqs. (3.3) - (3.6) of the form

$$(\phi, \psi, \phi_2, \phi^*) = [f(z), g(z), w(z), h(z)]e^{i\xi(x-ct)}, \quad (4.1)$$

where  $c = \frac{\omega}{\xi}$  is the non - dimensional phase velocity,  $\omega$  and  $\xi$  are respectively the circular frequency and wave number.

Using Eq.(4.1) in Eqs. (3.3) - (3.6) and solving the resulting differential equations, the expressions for  $\phi, \psi, \phi_2$  and  $\phi^*$  are obtained as

$$\phi = (A \cos m_1 z + B \sin m_1 z + C \cos m_2 z + D \sin m_2 z)e^{i\xi(x-ct)}, \quad (4.2)$$

$$\psi = (A' \cos m_3 z + B' \sin m_3 z + C' \cos m_4 z + D' \sin m_4 z)e^{i\xi(x-ct)}, \quad (4.3)$$

$$\phi_2 = \delta^2 [(b^2 - m_3^2)(A' \cos m_3 z + B' \sin m_3 z) + (b^2 - m_4^2)(C' \cos m_4 z + D' \sin m_4 z)]e^{i\xi(x-ct)}, \quad (4.4)$$

$$\phi^* = -\frac{1}{\delta_3^2} [(a^2 - m_1^2)(A \cos m_1 z + B \sin m_1 z) + (a^2 - m_2^2)(C \cos m_2 z + D \sin m_2 z)]e^{i\xi(x-ct)}. \quad (4.5)$$

where

$$m_i^2 = \xi^2(c^2 a_i^2 - 1), i = 1, 2, 3, 4; a^2 = \xi^2(c^2 - 1), b^2 = \xi^2\left(\frac{c^2}{\delta^2} - 1\right),$$

$$(a_1^2, a_2^2) = \frac{1}{2} \{ [1 + \delta_6^2 - \frac{1}{\omega^2}(\delta_4^2 - \delta_3^2 \delta_5^2)] \pm [1 - \delta_6^2 - \frac{1}{\omega^2}(\delta_4^2 - \delta_3^2 \delta_5^2)] \}^2 + \frac{4}{\omega^2} \{ \delta_4^2 + \delta_6^2(\delta_4^2 - \delta_3^2 \delta_5^2) \}^{\frac{1}{2}}$$

$$(a_3^2, a_4^2) = \frac{1}{2} \{ [\delta_2^2 + \frac{1}{\delta^2} + \frac{\delta^{*2}}{\omega^2 \delta^2} (1 - \frac{2\delta_2^2 \delta^2}{\delta^{*2}})] \pm [ \frac{1}{\delta^2} - \delta_2^2 + \frac{\delta^{*2}}{\omega^2 \delta^2} (1 - \frac{2\delta_2^2 \delta^2}{\delta^{*2}})] \}^2 + \frac{4\delta_2^2}{\omega^2 \delta^2} \{ \delta^{*2} - 2(\delta^2 \delta_2^2 - 1) \}^{\frac{1}{2}}$$

With the help of equations (3.2), (4.2) and (4.3) we obtain the displacement

components  $u_1$  and  $u_3$  as

$$u_1 = [\iota\xi(A \cos m_1 z + B \sin m_1 z + C \cos m_2 z + D \sin m_2 z) + (-A' m_3 \sin m_3 z + B' m_3 \cos m_3 z - C' m_4 \sin m_4 z + D' m_4 \cos m_4 z)] e^{\iota\xi(x-ct)} \quad (4.6)$$

$$u_3 = [(-m_1 A \sin m_1 z + m_1 B \cos m_1 z - m_2 C \sin m_2 z + m_2 D \cos m_2 z) - \xi(A' \cos m_3 z + B' \sin m_3 z + C' \cos m_4 z + D' \sin m_4 z)] e^{\iota\xi(x-ct)}. \quad (4.7)$$

## 5 Derivation of the Secular Equations

Invoking the boundary conditions (3.7) on the surfaces  $z = \pm d$  of the plate and using Eqs. (4.2) - (4.7), we obtain a system of eight simultaneous Eqs.

$$P(AC_1 + Bs_1 + CC_2 + Ds_2) + Q\{m_3(A's_3 - B'C_3) + m_4(C's_4 - D'C_4)\} = 0, \quad (5.1)$$

$$P(AC_1 - Bs_1 + CC_2 - Ds_2) + Q\{m_3(-A's_3 - B'C_3) + m_4(-C's_4 - D'C_4)\} = 0, \quad (5.2)$$

$$Q\{(-As_1 + BC_1)m_1 + (-Cs_2 + DC_2)m_2\} + P(A'C_3 + B's_3 + C'C_4 + D's_4) = 0, \quad (5.3)$$

$$Q\{(As_1 + BC_1)m_1 + (Cs_2 + DC_2)m_2\} + P(A'C_3 - B's_3 + C'C_4 - D's_4) = 0, \quad (5.4)$$

$$R[g_1 C_1 A + g_1 s_1 B + g_2 C_2 C + g_2 s_2 D] + S[f_3(-A's_3 + B'C_3)m_3 + f_4(-C's_4 + D'C_4)m_4] = 0, \quad (5.5)$$

$$R[g_1 C_1 A - g_1 s_1 B + g_2 C_2 C - g_2 s_2 D] + S[f_3(A's_3 + B'C_3)m_3 + f_4(C's_4 + D'C_4)m_4] = 0, \quad (5.6)$$

$$U[g_1(-Am_1 s_1 + Bm_1 C_1) + g_2(-Cm_2 s_2 + Dm_2 C_2) - V[f_3 C_3 A' + f_3 s_3 B' + f_4 C_4 C' + f_4 s_4 D']] = 0, \quad (5.7)$$

$$U[g_1(Am_1 s_1 + Bm_1 C_1) + g_2(Cm_2 s_2 + Dm_2 C_2) - V[f_3 C_3 A' - f_3 s_3 B' + f_4 C_4 C' - f_4 s_4 D']] = 0, \quad (5.8)$$

where

$$P = b^2 - \xi^2 + \frac{p\xi^2}{\delta^2}, Q = -2\iota\xi\left(1 - \frac{p}{2\delta^2}\right), R = \frac{\iota\xi b_0 I}{\delta^3}, S = \gamma_I \delta^2, U = \frac{\alpha_0 I}{\delta^3},$$

$$V = \iota \xi b_{0I} \delta^2, f_i = b^2 - m_i^2, i = 3, 4; g_i = a^2 - m_i^2, i = 1, 2;$$

$$s_i = \sin m_i d, C_i = \cos m_i d, i = 1, 2, 3, 4.$$

The system of Eqs. (5.1) - (5.8) has a non-trivial solution if the determinant of the coefficients of amplitudes  $[A, B, C, D, A', B', C', D']^T$  vanishes. We obtain the following secular equations after applying lengthy algebraic reductions and manipulations

$$\begin{aligned} & \left\{ 1 + \frac{QR(m_1^2 - a^2)}{PS(m_4^2 - b^2)} + \frac{QV(m_3^2 - b^2)}{PU(m_2^2 - a^2)} + \frac{Q^2RV(m_1^2 - a^2)(m_3^2 - b^2)}{P^2SU(m_2^2 - a^2)(m_4^2 - b^2)} \right\} \left[ \frac{\tan m_1 d}{\tan m_3 d} \right]^{\pm 1} \\ & - \left\{ \frac{m_1(m_1^2 - a^2)}{m_2(m_2^2 - a^2)} + \frac{QRm_1(m_1^2 - a^2)}{PSm_2(m_4^2 - b^2)} + \frac{QVm_1(m_3^2 - b^2)}{PUm_2(m_2^2 - a^2)} + \frac{Q^2RVm_1(m_3^2 - b^2)}{P^2SUm_2(m_4^2 - b^2)} \right\} \left[ \frac{\tan m_2 d}{\tan m_3 d} \right]^{\pm 1} \\ & - \left\{ \frac{m_3(m_3^2 - b^2)}{m_4(m_4^2 - b^2)} + \frac{QRm_3(m_1^2 - a^2)}{PSm_4(m_4^2 - b^2)} + \frac{QVm_3(m_3^2 - b^2)}{PUm_4(m_2^2 - a^2)} + \frac{Q^2RVm_3(m_1^2 - a^2)}{P^2SUm_4(m_2^2 - a^2)} \right\} \left[ \frac{\tan m_1 d}{\tan m_4 d} \right]^{\pm 1} \\ & + \left\{ \frac{m_1m_3(m_1^2 - a^2)(m_3^2 - b^2)}{m_2m_4(m_2^2 - a^2)(m_4^2 - b^2)} + \frac{QRm_1m_3(m_1^2 - a^2)}{PSm_2m_4(m_4^2 - b^2)} + \frac{QVm_1m_3(m_3^2 - b^2)}{PUm_2m_4(m_2^2 - a^2)} \right. \\ & \left. + \frac{Q^2RVm_1m_3}{P^2SUm_2m_4} \right\} \left[ \frac{\tan m_2 d}{\tan m_4 d} \right]^{\pm 1} - \frac{RV(m_2^2 - m_1^2)(m_4^2 - m_3^2)}{SU(m_4^2 - b^2)(m_2^2 - a^2)} \left[ \frac{\tan m_1 d}{\tan m_3 d} \right] \left[ \frac{\tan m_2 d}{\tan m_4 d} \right]^{\pm 1} \\ & = \frac{-4\xi^2 \left(1 - \frac{p}{2\delta^2}\right)^2 m_1 m_3 (m_2^2 - m_1^2) (m_4^2 - m_3^2)}{(b^2 - \xi^2 + \frac{p\xi^2}{\delta^2})^2 (m_4^2 - b^2) (m_2^2 - a^2)} \end{aligned} \quad (5.9)$$

Here the exponent +1 refers to skew-symmetric and -1 refers to symmetric modes of wave propagation.

## 5.1 Particular cases

### 5.1.1 Micropolar elastic Plate

In the absence of viscous effect ( $\alpha_{0I} = \lambda_{0I} = \lambda_{1I} = 0$ ) and microstretch effect ( $\alpha_0 = \lambda_0 = \lambda_1 = b_0 = 0$ ), the secular equation (5.9) reduces to

$$\left[ \frac{\tan m_1 d}{\tan m_3 d} \right]^{\pm 1} - \frac{m_3(b^2 - m_3^2)}{m_4(b^2 - m_4^2)} \left[ \frac{\tan m_1 d}{\tan m_4 d} \right]^{\pm 1} = \frac{-4\xi^2 \left(1 - \frac{p}{2\delta^2}\right)^2 am_3(m_4^2 - m_3^2)}{(b^2 - \xi^2 + \frac{p\xi^2}{\delta^2})^2 (m_4^2 - b^2)} \quad (5.10)$$

The equation (5.10) agrees with Kumar and Partap [17] and has been discussed for homogeneous, isotropic, stress-free micropolar elastic plate.

### 5.1.2 Elastic Plate

In the absence of micropolarity effect ( $K = p = 0$ ), the secular equation (5.10) reduces to

$$\left[ \frac{\tan m_1 d}{\tan m_3 d} \right]^{\pm 1} = \frac{-4\xi^2 ab}{(b^2 - \xi^2)^2} \quad (5.11)$$

The equation (5.11) agrees with Graff [6] and has been discussed for homogeneous, isotropic, stress-free elastic plate.

## 6 Regions of the Secular Equation

In order to explore various regions of the secular equations, here we consider the equation (5.9) as an example for the purpose of discussion. Depending upon whether  $m_1, m_2, m_3, m_4, a, b$  being real, purely imaginary or complex, the frequency equation (5.9) is correspondingly altered as follows:

### 6.1 Region I

When the characteristic roots are of the type,  $a^2 = -\alpha'^2, b^2 = -\beta'^2, m_k^2 = -\alpha_k^2, k = 1, 2, 3, 4$  so that  $a = i\alpha', b = i\beta', m_k = i\alpha_k, k = 1, 2, 3, 4$  are purely imaginary or complex numbers. This ensures that the superposition of partial waves has the property of exponential decay. In this case, the secular equations are written from equation (5.9) by replacing circular tangent functions of  $m_k, k = 1, 2, 3, 4$  with hyperbolic tangent functions of  $\alpha_k, k = 1, 2, 3, 4$ .

### 6.2 Region II

This region is characterized by  $\delta < c < 1$ . In this case, we have  $b = b, m_3 = m_3, m_4 = m_4, a = i\alpha', m_k = i\alpha_k (i = 1, 2)$  and the secular equations can be obtained from equation (5.9) by replacing circular tangent functions of  $m_k, k = 1, 2$  with hyperbolic tangent functions of  $\alpha_k, k = 1, 2$ .

### 6.3 Region III

In this case, the characteristic roots are given by  $m_k^2, k = 1, 2, 3, 4$  and the secular equation is given by equation (5.9).

## 7 Waves of Short Wavelength

Some information on the asymptotic behavior is obtained by letting  $\xi \rightarrow \infty, \frac{\tanh \alpha_i d}{\tanh \alpha_j d} \rightarrow 1, i = 1, 2; j = 3, 4$ . If we take  $\xi > \frac{\omega}{\delta}$ , it follows that

$c < \delta, 1$ . Then we replace  $a, b, m_i$  with  $\iota\alpha', \iota\beta', \iota\alpha_i$  and secular equations (5.9) reduces to

$$\begin{aligned} & 4\xi^2\left(1 - \frac{p}{2\delta^2}\right)^2 \alpha_1\alpha_2\alpha_3\alpha_4(\alpha_1 + \alpha_2)(\alpha_3 + \alpha_4) \\ = & \left(\frac{p\xi^2}{\delta^2} - \beta'^2 - \xi^2\right)^2 [(\alpha_1^2 + \alpha_2^2 + \alpha_1\alpha_2 - \alpha'^2)(\alpha_3^2 + \alpha_4^2 + \alpha_3\alpha_4 - \beta'^2) \\ & + \frac{QR}{PS}(\alpha_1^2 - \alpha'^2)(\alpha_2^2 - \alpha'^2) + \frac{QV}{PU}(\alpha_3^2 - \beta'^2)(\alpha_4^2 - \beta'^2) \\ & + \frac{Q^2RV}{P^2SU}(\alpha_3\alpha_4 + \beta'^2)(\alpha_1\alpha_2 + \alpha'^2) - \frac{RV}{SU}(\alpha_1 + \alpha_2)(\alpha_3 + \alpha_4)]. \end{aligned}$$

These are merely Rayleigh surface wave equations. The Rayleigh results enter here since for such wavelengths, the finite thickness plate appears as a half-space. Hence vibrational energy is transmitted mainly along the surface of the plate.

## 8 Lamé Modes

A special class of exact solutions, called the Lamé modes, but evidently first identified by Lamb[5] can be obtained by considering the special case  $b^2 = \xi^2\left(1 - \frac{p}{\delta^2}\right)$ , the roots for this case are in Region II and the frequency equation (5.9) reduces to

Symmetric modes:  $\tan m_3d = \infty, \Rightarrow m_3 = \frac{n\pi}{2d}, n = 1, 3, 5, \dots$

Anti symmetric modes:  $\tan m_3d = 0, \Rightarrow m_3 = \frac{n\pi}{2d}, n = 0, 2, 4, \dots$

Here, the frequency is given by

$$\omega = \frac{\sqrt{4b^2d^2 + n^2\pi^2\left(1 - \frac{p}{\delta^2}\right)}}{2da_3\sqrt{1 - \frac{p}{\delta^2}}}$$

## 9 Amplitudes of Displacements, Microrotation and Microstretch

In this section the amplitudes of displacement components, microrotation and microstretch for symmetric and skew-symmetric modes of plate waves, have been computed. Upon using Eqs. (4.2) - (4.7), we obtain

$$\begin{aligned}
(u_1)_{sym} &= \{\iota\xi(\cos m_1 z + L \cos m_2 z) + M m_3 \cos m_3 z + N m_4 \cos m_4 z\} A e^{\iota\xi(x-ct)}, \\
(u_1)_{asym} &= \{\iota\xi(\sin m_1 z + L' \sin m_2 z) + M' m_3 \sin m_3 z + N' m_4 \sin m_4 z\} B e^{\iota\xi(x-ct)}, \\
(u_3)_{sym} &= -\{m_1 \sin m_1 z + L m_2 \sin m_2 z + \iota\xi(M \sin m_3 z + N \sin m_4 z)\} A e^{\iota\xi(x-ct)}, \\
(u_3)_{asym} &= \{m_1 \cos m_1 z + L' m_2 \cos m_2 z + \iota\xi(M' \cos m_3 z + N' \cos m_4 z)\} B e^{\iota\xi(x-ct)}, \\
(\phi_2)_{sym} &= \delta^2 \{(b^2 - m_3^2) \sin m_3 z - (b^2 - m_4^2) \frac{f_3 m_3 C_3}{f_4 m_4 C_4} \sin m_4 z\} B' e^{\iota\xi(x-ct)}, \\
(\phi_2)_{asym} &= \delta^2 \{(b^2 - m_3^2) \cos m_3 z - (b^2 - m_4^2) \frac{f_3 m_3 s_3}{f_4 m_4 s_4} \cos m_4 z\} A' e^{\iota\xi(x-ct)}, \\
(\phi^*)_{sym} &= \frac{1}{\delta_3^2} \{(a^2 - m_1^2) \cos m_1 z + (a^2 - m_2^2) L \cos m_2 z\} A e^{\iota\xi(x-ct)}, \\
(\phi^*)_{asym} &= \frac{1}{\delta_3^2} \{(a^2 - m_1^2) \sin m_1 z + (a^2 - m_2^2) L' \sin m_2 z\} B e^{\iota\xi(x-ct)}.
\end{aligned}$$

where

$$\begin{aligned}
L &= -\frac{g_1 m_1 s_1}{g_2 m_2 s_2}, \quad L' = -\frac{g_1 m_1 C_1}{g_2 m_2 C_2}, \\
M &= \frac{P(g_2 m_2 T_1^{-1} - g_1 m_1 T_2^{-1}) f_4 s_1}{Q g_2 m_2 m_3 (f_4 - f_3) T_3^{-1} s_3}, \quad M' = \frac{P(g_2 m_2 T_1 - g_1 m_1 T_2) f_4 C_1}{Q g_2 m_2 m_3 (f_4 - f_3) T_3 C_3}, \\
N &= -\frac{P(g_2 m_2 T_1^{-1} - g_1 m_1 T_2^{-1}) f_3 s_1}{Q g_2 m_2 m_4 (f_4 - f_3) T_4^{-1} s_4}, \quad N' = -\frac{P(g_2 m_2 T_1 - g_1 m_1 T_2) f_3 C_1}{Q g_2 m_2 m_4 (f_4 - f_3) T_4 C_4},
\end{aligned}$$

$$T_i = \tan m_i d, \quad i = 1, 2, 3, 4.$$

## 10 Example results

With the view of illustrating theoretical results obtained in the preceding sections, we now present some numerical results. The material chosen for this purpose is Aluminium-epoxy composite (microstretch elastic solid), the physical data for which is given below

$$\rho = 2.19 \times 10^3 \text{ Kg m}^{-3}, \quad \lambda = 7.59 \times 10^9 \text{ Nm}^{-2}, \quad \mu = 1.89 \times 10^9 \text{ Nm}^{-2},$$

$$K = 0.0149 \times 10^9 \text{ Nm}^{-2}, \quad \gamma = 0.0268 \times 10^5 \text{ N}, \quad j = 0.00196 \times 10^{-4} \text{ m}^2,$$

$$j_0 = 0.00185 \times 10^{-4} \text{ m}^2, \quad \lambda_0 = \lambda_1 = 0.037 \times 10^9 \text{ Nm}^{-2}, \quad \alpha_0 = 0.61 \times 10^{-5} \text{ N},$$

$$b_0 = 0.025 \times 10^5 N, d = 0.01m.$$

For a particular model of a microstretch viscoelastic solid, the relevant parameters following Kumar and Singh [16] are expressed as

$\chi_I = \chi(1 - \nu Q_k^{-1})$ ,  $k = 1, 2, 3, 4, 5, 6, 7, 8$  for  $\chi = \lambda, \mu, K, \gamma, \alpha_0, \lambda_0, \lambda_1, b_0$  respectively where  $Q_1^{-1} = 0.05, Q_2^{-1} = 0.01, Q_3^{-1} = 0.015, Q_4^{-1} = 0.1, Q_5^{-1} = 0.15, Q_6^{-1} = 0.15, Q_7^{-1} = 0.1, Q_8^{-1} = 0.1$ .

A FORTRAN program has been developed for the solution of equation (5.9) to compute phase velocity  $c$  for different values of  $n$  by using the relations  $\tan(\theta) = \tan(n\pi + \theta)$  and  $m_i^2 = \xi^2(c^2 a_i^2 - 1)$ .

In general, wave number and phase velocity of the waves are complex quantities, therefore, the waves are attenuated in space. If we write

$$c^{-1} = v^{-1} + i\omega^{-1}q \quad (10.1)$$

then  $\xi = K_1 + i q$ , where  $K_1 = \frac{\omega}{v}$  and  $q$  are real numbers. This shows that  $v$  is the propagation speed and  $q$  is attenuation coefficient of waves. Upon using Eq.(10.1) in the FORTRAN program developed for the solution of equation (5.9) to compute phase velocity  $c$ , attenuation coefficient  $q$  for different modes of wave propagation can be obtained.

The non-dimensional phase velocity and attenuation coefficient of symmetric and skew-symmetric modes of wave propagation have been computed for various values of non-dimensional wave number from secular equation (5.9). The corresponding numerically computed values of phase velocity and attenuation coefficient are shown graphically in Figs. 2-5 for different modes ( $n = 0$  to  $n = 3$ ). The amplitudes of displacements, microrotation and microstretch for symmetric and skew-symmetric modes are presented graphically in Figs. 6-13. The solid curves correspond to microstretch viscoelastic plate (MVEP) and dotted curves refer to microstretch elastic plate (MEP).

### 10.1 Phase velocity

The phase velocity of higher modes of wave propagation, symmetric and skew-symmetric attains quite large values at vanishing wave number, which sharply slashes down to become steady with increasing wave number. It is observed that the phase velocities of different modes of wave propagation start from large values at vanishing wave number and then exhibit strong dispersion until the velocity flattens out to the value of the microstretch Rayleigh wave velocity of the material at higher wave numbers. The reason

for this asymptotic approach is that for short wavelengths (or high frequencies) the material plate behaves increasingly like a thick slab and hence the coupling between upper and lower boundary surfaces is reduced and as a result the properties of symmetric and skew-symmetric waves become more and more similar.

The phase velocity of lowest symmetric and skew-symmetric mode ( $n = 0$ ) remains constant with the variation in wave number in microstretch elastic plate (MEP) and microstretch viscoelastic plate (MVEP) respectively, whereas the phase velocity of lowest symmetric mode and skew-symmetric mode ( $n = 0$ ) varies at lower wave number and becomes constant at higher wave number in microstretch viscoelastic plate (MVEP) and microstretch elastic plate (MEP) respectively.

It is observed that phase velocity in MEP is more than in MVEP for symmetric modes  $n = 1, 2, 3$  and skew-symmetric modes  $n = 0, 1, 2, 3$ . In case of lowest symmetric mode ( $n = 0$ ), for wave number  $\xi \leq 0.8$  phase velocity in MVEP is more than in case of MEP, the values of phase velocity are smaller in MVEP than in MEP for wave number  $\xi \geq 0.8$ . The phase velocity for symmetric mode  $n = 2$  in MEP is more than in case of MVEP for symmetric mode  $n = 3$ .

## 10.2 Attenuation coefficients

The variation of attenuation coefficient with wave number for symmetric and skew-symmetric modes is represented graphically in Figs. 3 and 5 respectively in case of microstretch viscoelastic plate (MVEP). For the symmetric modes  $n = 1, 2, 3$ , we observe the following

(i) the magnitude of attenuation coefficient has maxima upto 10.14 at  $\xi = 5.07$ . (ii) The variation of attenuation coefficient with wave number remains same. (iii) the attenuation coefficient varies linearly with wave number. For lowest symmetric mode  $n = 0$ , the magnitude of attenuation coefficient increases upto 8.37 in region  $0.07 \leq \xi \leq 3.08$  at  $\xi = 1.08$  and varies linearly with increase in wave number and attains maxima upto 10.13 in region  $3.08 \leq \xi \leq 5.07$  at  $\xi = 5.07$ .

For skew-symmetric modes we observe the following (i) the attenuation coefficient varies linearly with wave number for modes  $n = 2, 3$  (ii) for mode  $n = 1$ , the attenuation coefficient varies linearly with wave number in region  $0.07 \leq \xi \leq 4.08$  and the attenuation coefficient is highest in the region  $4.08 \leq \xi \leq 5.08$  and attains maximum value upto 10.89 at  $\xi = 5.08$  (iii) for lowest mode, the attenuation coefficient varies linearly with wave number in region  $1.08 \leq \xi \leq 5.08$  and the lowest mode has higher attenuation

coefficient than other modes for the region  $0.07 \leq \xi \leq 1.08$

### 10.3 Amplitudes

Figs. 6-13 depict the variations of symmetric and skew-symmetric amplitudes of displacement ( $u_1$ ), displacement ( $u_3$ ), microrotation ( $\phi_2$ ) and microstretch ( $\phi^*$ ) in case of microstretch viscoelastic plate (MVEP) and microstretch elastic plate (MEP). The displacement ( $u_1$ ) of the plate is maximum at the centre and minimum at the surfaces for symmetric mode as can be seen from Fig.6. It is evident from Fig. 7 and Fig. 8 that (i) the values of the skew-symmetric displacement ( $u_1$ ) and symmetric displacement ( $u_3$ ) of the plate is maximum at top surface, zero at the centre and minimum at the bottom surface in case of microstretch elastic plate (MEP) (ii) the values of the skew-symmetric displacement ( $u_1$ ) is minimum at  $z = -0.6d$ , zero at the centre and maximum at  $z = 0.6d$ , whereas the values of the symmetric displacement is maximum at  $z = -0.6d$ , zero at the centre and minimum at  $z = 0.6d$  in case of microstretch viscoelastic plate (MVEP). From Fig.9, it is noticed that the values of the displacement ( $u_3$ ) of the plate is maximum at the centre and minimum at the surfaces in case of microstretch viscoelastic plate (MVEP) and minimum at the centre and maximum at the surfaces in case of microstretch elastic plate (MEP) for skew-symmetric mode. The values of the symmetric microrotation ( $\phi_2$ ) of the plate is maximum at top surface, zero at the centre and minimum at the bottom surface as seen from Fig. 10. The values of the microrotation ( $\phi_2$ ) and microstretch ( $\phi^*$ ) of the plate is minimum at the centre and maximum at the surfaces for skew-symmetric mode and symmetric modes respectively as observed from Fig.11 and Fig. 12. The values of the skew-symmetric microstretch ( $\phi^*$ ) of the plate is minimum at top surface, zero at the centre and maximum at the bottom surface as seen from Fig. 13.  $(u_1)_{sym}$ ,  $(u_1)_{asym}$ ,  $(u_3)_{sym}$ ,  $(u_3)_{asym}$ ,  $(\phi_2)_{sym}$ ,  $(\phi_2)_{asym}$ ,  $(\phi^*)_{sym}$  and  $(\phi^*)_{asym}$  correspond to the values of ( $u_1$ ), ( $u_3$ ), ( $\phi_2$ ) and ( $\phi^*$ ) for symmetric and skew-symmetric modes respectively. The values of the symmetric displacement ( $u_1$ ), skew-symmetric displacement ( $u_3$ ) and skew-symmetric microrotation ( $\phi_2$ ) of the plate are more in microstretch elastic plate (MEP) in comparison to microstretch viscoelastic plate (MVEP), whereas values of the symmetric microstretch ( $\phi^*$ ) of the plate are more in microstretch viscoelastic plate (MVEP) in comparison to microstretch elastic plate (MEP). The values of the skew-symmetric displacement ( $u_1$ ), symmetric displacement ( $u_3$ ) and symmetric microrotation ( $\phi_2$ ) of the plate are smaller in microstretch elastic plate (MEP) in comparison to microstretch viscoelastic plate (MVEP)

below the centre of the plate and are more in microstretch elastic plate (MEP) in comparison to microstretch viscoelastic plate (MVEP) above the centre of the plate, whereas the values of the skew-symmetric microstretch ( $\phi^*$ ) of the plate in case of microstretch elastic plate (MEP) are more below the centre of the plate and are smaller above the centre of the plate.

## 11 Conclusions

(i) The propagation of free vibrations in infinite homogeneous, isotropic microstretch viscoelastic plate subjected to stress-free conditions is investigated after deriving the secular equations (ii) It is noticed that the motion of free vibrations is governed by the Rayleigh - Lamb type secular equations (iii) At short wavelength limit, the secular equations in case of symmetric and skew-symmetric modes of propagation of free vibrations in a stress-free plate reduces to the Rayleigh surface frequency equations (iv) The phase velocities of higher modes of propagation, symmetric and skew-symmetric attain quite large values at vanishing wave number which sharply slashes down to become steady and asymptotic to the reduced Rayleigh wave velocity with increasing wave number. The phase velocity in MEP is more than in MVEP for symmetric modes  $n = 1, 2, 3$  and skew-symmetric modes  $n = 0, 1, 2, 3$  (v) The attenuation coefficient varies linearly with wave number for symmetric modes  $n = 1, 2, 3$  and for skew-symmetric modes  $n = 2, 3$  (vi) The amplitudes of displacement components, microrotation and microstretch for symmetric and skew-symmetric modes are computed numerically and presented graphically.

## References

- [1] A. C. Eringen, Linear theory of micropolar viscoelasticity, *Int. J. Engng. Sci.*, 5(1967), 191-204.
- [2] A. C. Eringen, *Micropolar elastic solids with stretch*, Ari Kitabevi Matbassi, Istanbul, 1971.
- [3] A. C. Eringen, Theory of thermo-microstretch elastic solids, *Int. J. Engng. Sci.*, 28(1990), 1291-1301.
- [4] A. C. Eringen, *Microcontinuum field theories I: Foundations and Solids*, Springer - Verlag, New York, 1999.

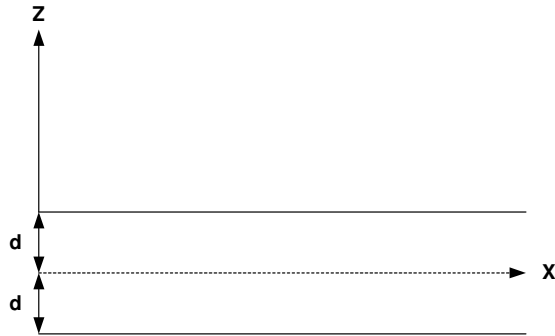
- [5] H. Lamb, On waves in an elastic plate, *Phil. Trans.Roy. Soc., London*, 93(1917), 114-128.
- [6] K. F. Graff, *Wave motion in Elastic Solids*, Dover publications, New York, 1991.
- [7] M. F. McCarthy and A. C. Eringen, Micropolar viscoelastic waves, *Int. J. Engng. Sci.*, 7(1969), 447-458.
- [8] M. Svanadze, Fundamental solution of the system of equations of steady oscillations in the theory of microstretch elastic solids, *Int. J. Engng. Sci.*, 42(2004), 1897-1910.
- [9] P. K. Biswas, P. R. Sengupta and L. Debnath, Axisymmetric Lamb's problem in a semi-infinite micropolar viscoelastic medium, *Int. Math. Math. Sci.*, 19(1996), 815-820.
- [10] R. D. Gauthier, Experimental investigations of micropolar media, In: Brulin O, Hsieh R K T(eds). , *Mechanics of micropolar media*, Singapore (1982), 395-463.
- [11] R. Kumar , M. L. Gogna and L. Debnath , Lamb's plane problem in micropolar viscoelastic half space with stretch, *Int. J. Math. And Sci.*, 13(1990), 363-372.
- [12] R. Kumar and B. Singh, Reflection of plane waves at a planar viscoelastic micropolar interface, *Indian J. Pure and Applied Math.*, 31(2000), 287-303.
- [13] R. Kumar, Wave propagation in a micropolar viscoelastic generalized thermoelastic solid, *Int. J. Engng. Sci.*, 38(2000), 1377-1395.
- [14] R. Kumar, R. Singh and T. K. Chadha, Axisymmetric problem in microstretch elastic solids , *Indian Journal of Mathematics*, 44(2002), 147-164.
- [15] R. Kumar, R. Singh and T. K. Chadha, Plane strain problem in microstretch elastic solid , *Sadhana*, 28(2003), 975-990.
- [16] R. Kumar and R. Singh, Elastodynamics of an axisymmetric problem in microstretch viscoelastic solid , *Int. J. Applied Mechanics and Engineering*, 10(2005), 227-244.

- [17] R. Kumar and G. Partap, Reflection of plane waves in a heat flux dependent microstretch thermoelastic solid half space , *Int. J. of Applied Mechanics and Engineering*, 10(2005), 253-266.
- [18] R. Kumar and G. Partap, Rayleigh Lamb waves in micropolar isotropic elastic plate, *Applied Mathematics and Mechanics*, 27(2006), 1049-1059.
- [19] R. Kumar and G. Partap, Analysis of free vibrations for Rayleigh Lamb waves in a micropolar viscoelastic plate , *Int. J. of Applied Mechanics and Engineering*, 13(2008), 383-397.
- [20] R. Kumar and N. Sharma, Propagation of waves in micropolar viscoelastic generalized thermoelastic solids having interfacial imperfections , *Theoretical and Applied Fracture Mechanics* , 50(2008), 226-234.
- [21] S. De Cicco and L. Nappa, On Saint's Venant's principle for micropolar viscoelastic bodies , *Bit. J. Eng. Sci.*, 36(1998), 883-893.
- [22] S. De Cicco, Stress concentration effects in microstretch elastic solids , *Int. J. Engng. Sci.*, 41(2003), 187-199.
- [23] S. Ahmed EI - Karamany, Uniqueness and reciprocity theorems in generalized linear micropolar thermoviscoelasticity , *Int. J. Engng. Sci.*, 40(2003), 2097-2117.
- [24] X. Liu, and G. Hu, Inclusion problem of microstretch continuum, *Int. J. Engng. Sci.*, 42(2004), 849-860.

(Received 13 June 2008)

Rajneesh Kumar  
Department of Mathematics, Kurukshetra University,  
Kurukshetra 136 119 , INDIA.  
e-mail : rajneesh\_kuk @ rediffmail.com

Geeta Partap  
Department of Mathematics,  
Dr. B. R. Ambedkar National Institute of Technology,  
Jalandhar 144011, INDIA  
e-mail : gp.recjal@gmail.com and pratapg@nitj.ac.in

**Fig.1** Geometry of the problem

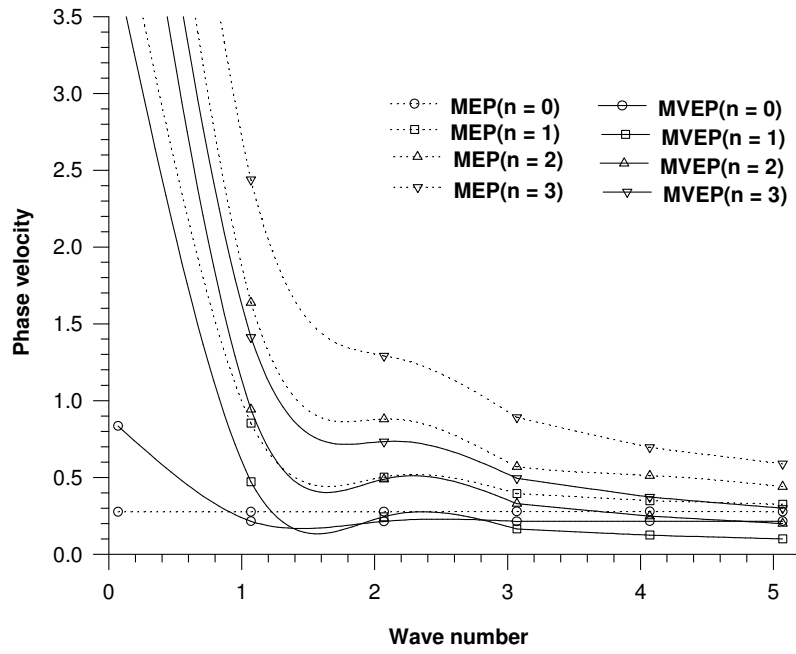


Fig. 2 Variation of phase velocity for symmetric modes of wave propagation

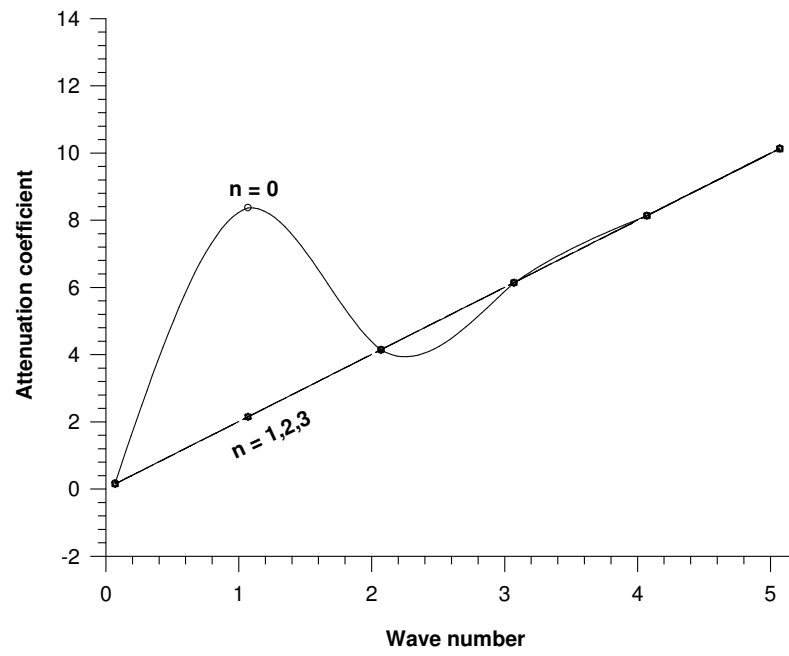


Fig. 3 Variation of attenuation coefficient of symmetric modes of wave propagation

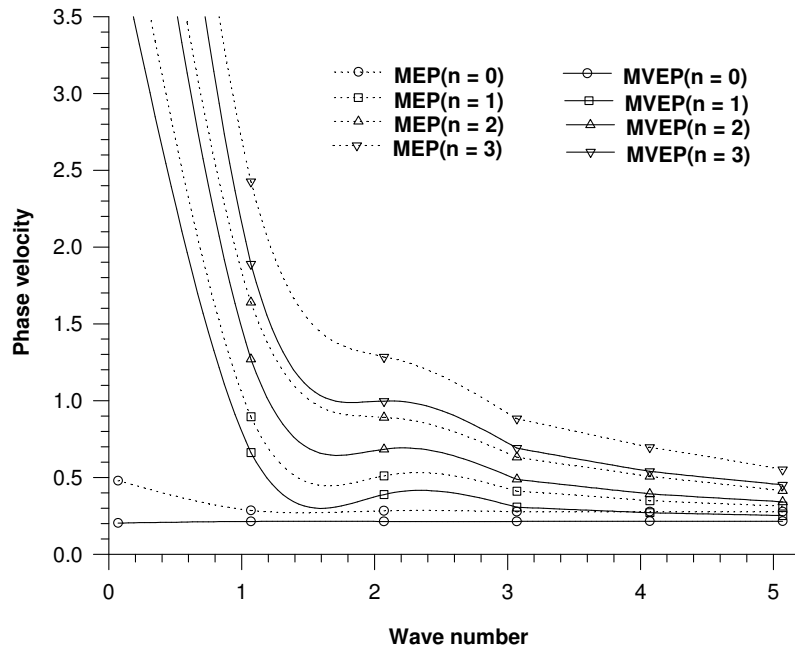
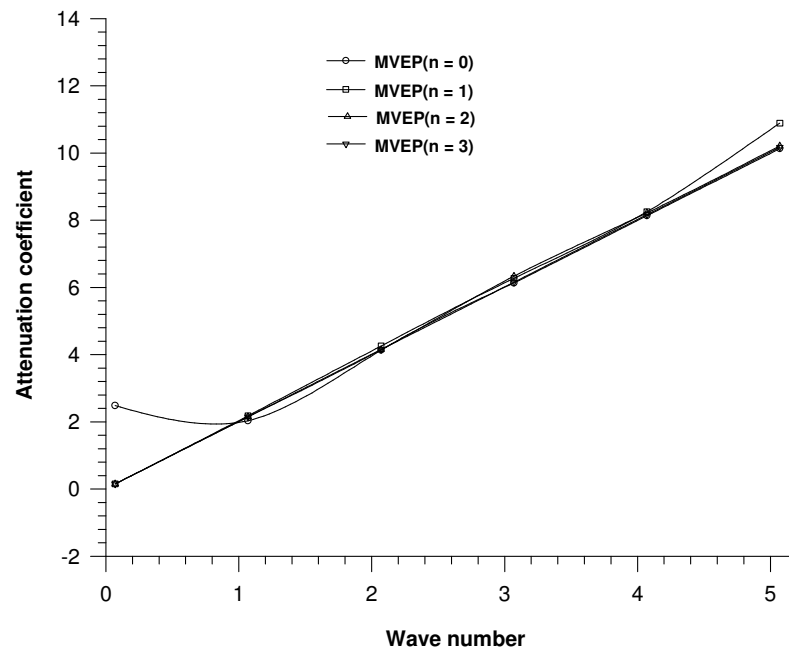


Fig. 4 Variation of phase velocity for skew-symmetric modes of wave propagation



**Fig. 5** Variation of attenuation coefficient of skew-symmetric modes of wave propagation

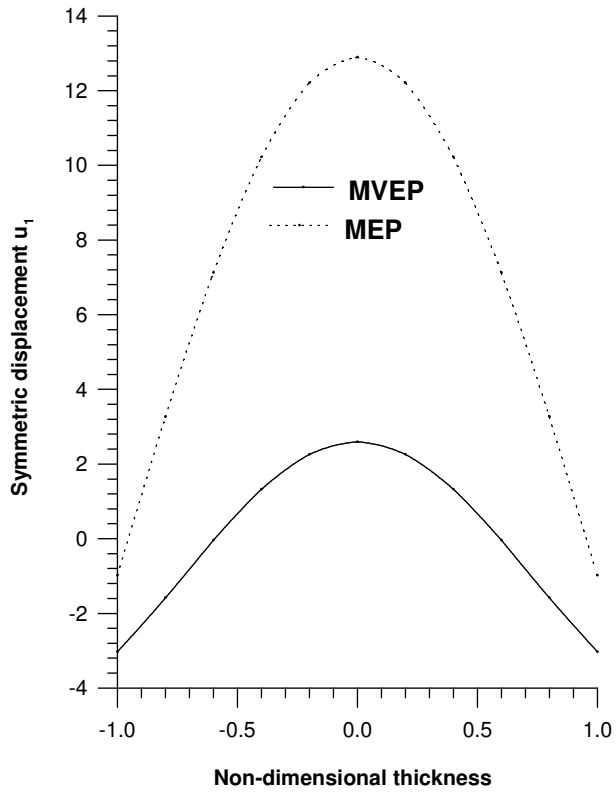


Fig. 6 Amplitude of symmetric displacement  $u_1$

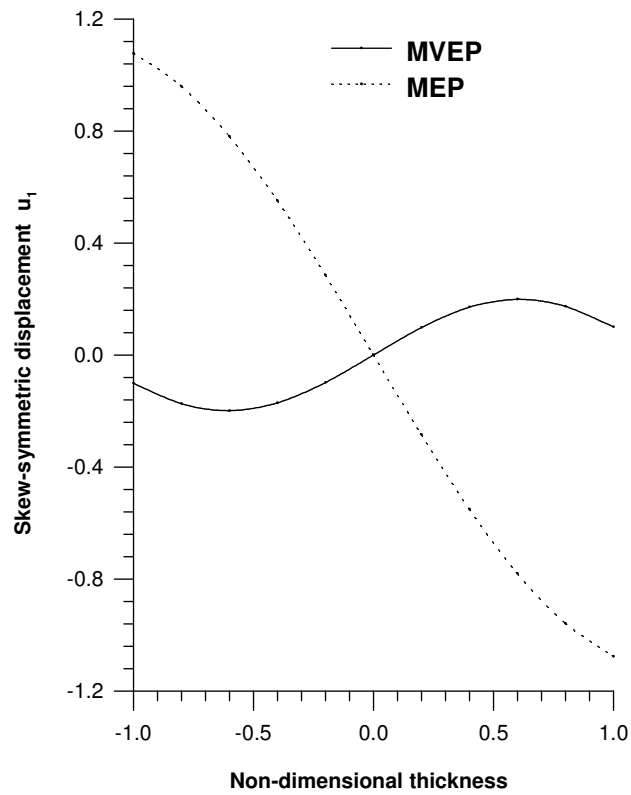


Fig. 7 Amplitude of skew-symmetric displacement  $u_1$

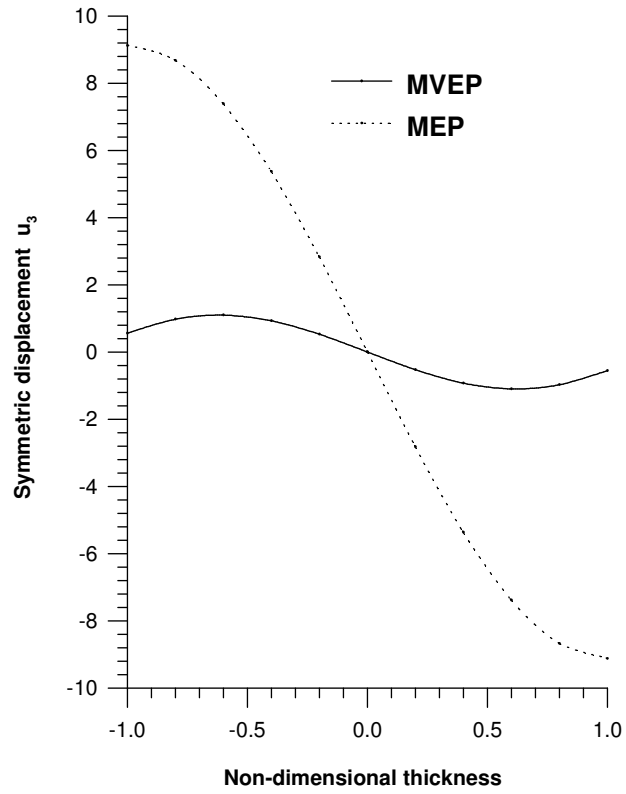


Fig. 8 Amplitude of symmetric displacement  $u_3$

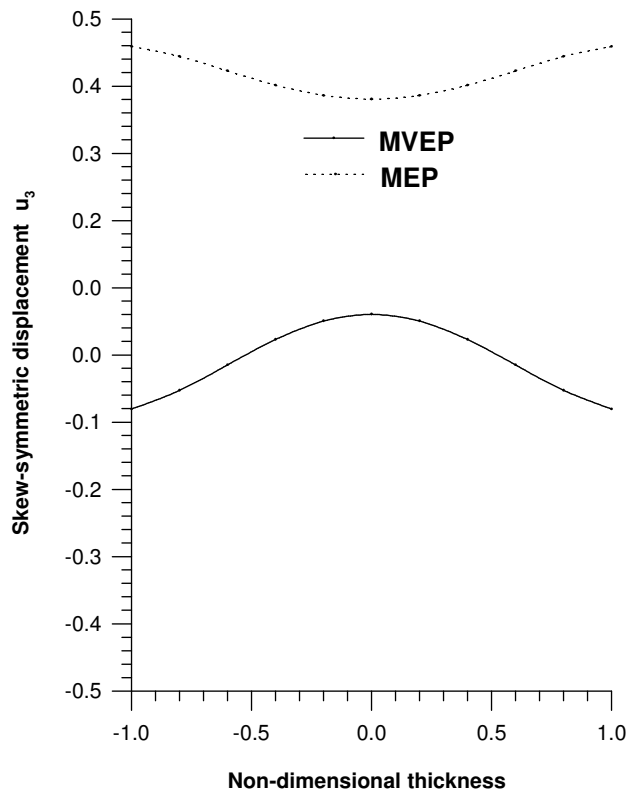


Fig. 9 Amplitude of skew-symmetric displacement  $u_3$

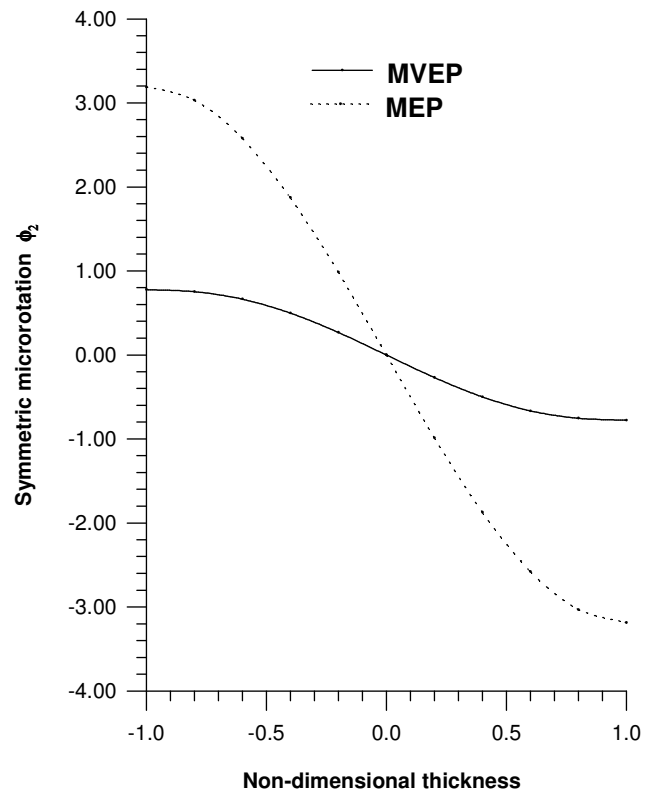


Fig. 10 Amplitude of symmetric microrotation  $\phi_2$

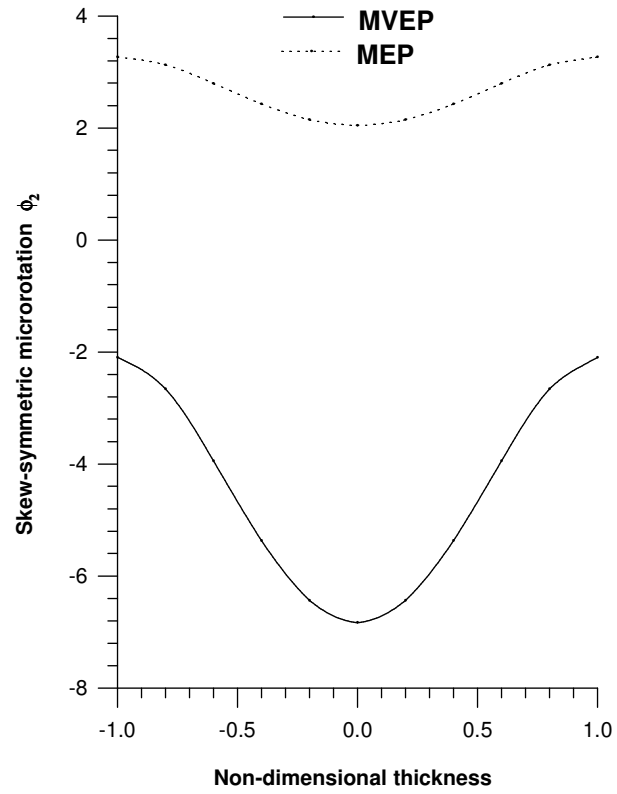


Fig. 11 Amplitude of skew-symmetric microrotation  $\phi_2$

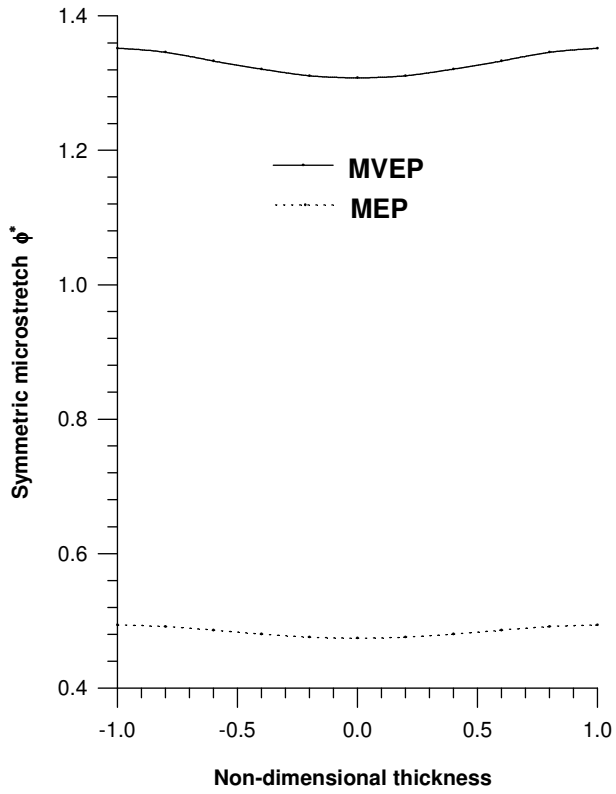


Fig. 12 Amplitude of symmetric microstretch  $\phi^*$

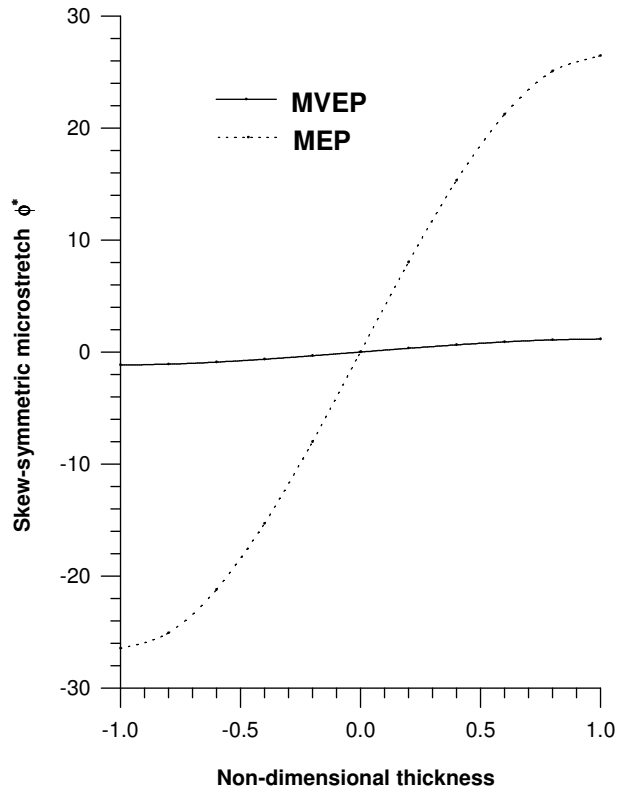


Fig. 13 Amplitude of skew-symmetric microstretch  $\phi^*$